Growth Mechanism and Threshold of Mode II and Mode III Fatigue Crack

Yukitaka MURAKAMI[1], Ryosuke KUSUMOTO[1], Koji TAKAHASHI[2]

[1]Department of Mechanical Engineering Science, Kyushu University, Higashi-ku, Fukuoka, 812-8581, Japan.
[2]Department of Energy and Safety Engineering, Yokohama National University, Hodogaya-ku, Yokohama, 240-8501, Japan.

ABSTRACT: *In order to make clear the relationship between ΔK_{IIth} and ΔK_{IIIth} and the influence of the rolling texture, Mode II and Mode III fatigue crack growth tests were carried out for annealed 0.47 % carbon steels (JIS S45C).The values of ΔK_{IIth} (9.5 MPa$\sqrt{m}$ and 9.7 MPa$\sqrt{m}$) for crack growth normal to the rolling direction were higher than the values of ΔK_{IIth} (8.8 MPa$\sqrt{m}$ and 8.1 MPa$\sqrt{m}$) for crack growth parallel to the rolling direction. Mode II and Mode III fatigue crack growth produced darkly etched microstructural layers in the vicinity of Mode II and Mode III fatigue crack. Vickers hardness of the layers was much higher than that of the original matrix (Mode II: HV 164 → HV 468. Mode III: HV 175 → HV 678). The layers consisted of very fine grains with the size ranging from 100 to 200 nm. The value of ΔK_{IIth} was approximately equal to ΔK_{IIIth}, i.e. $\Delta K_{IIth} \cong \Delta K_{III\ th} \cong 9.6$ MPa$\sqrt{m}$ for crack growth perpendicular to rolling direction. Therefore, the mechanism of Mode II fatigue crack growth is presumed to be essentially identical to that of Mode III fatigue crack growth.*

INTRODUCTION

There are many unsolved problems in Mode II [1-3] and Mode III [4-5] fatigue crack growth. For example, the correlation between the threshold stress intensity factor range for Mode II ΔK_{IIth} and that for Mode III $\Delta K_{\mathrm{IIIth}}$ has been unknown. The influence of the rolling texture of Mode II fatigue crack growth is also an unsolved problem. In this study, Mode II and Mode III fatigue crack growth tests were carried out on 0.47 % carbon steels and the value of ΔK_{IIth} and $\Delta K_{\mathrm{IIIth}}$ were measured. Mode II fatigue crack growth test specimens were taken in three different directions to the rolling direction. The influence of the rolling texture was investigated by comparing the Mode II and Mode III fatigue crack growth mechanism and threshold.

SPECIMEN AND EXPERIMENTAL METHOD

Material

Three 0.47 % C steels (JIS S45C) were used. Mode II fatigue crack growth test specimens were taken from the rolled bar with diameter of 60 mm and the rolled plate. Mode III fatigue crack growth test specimens were taken from the rolled bar with diameter of 25 mm. The specimens were machined after annealing at 844°C for 1 hr. After machining, the specimens were annealed in a vacuum at 600°C for 1 hr to relieve the residual stress induced by machining. After vacuum annealing, Vickers hardness *HV* was measured with a load of 0.98 N. Vickers hardness of the Mode II fatigue crack growth test specimen from the rolled bar is *HV* = 164, *HV* = 189 for the Mode II fatigue crack growth test specimen from the rolled plate, and *HV* = 175 for the Mode III fatigue crack growth test specimen.

Specimen and experimental method for Mode II fatigue crack growth test

Mode II fatigue crack growth tests were carried out by using the double cantilever (DC) specimen designed by Murakami and Hamada [1-3].

Figure 1 shows the shape and dimensions of the specimen. In order to measure ΔK_{IIth} by this method, three series of specimens which were cut from three different directions to the rolling direction were used.

Figure 2 shows the directions of cutting specimens from the rolled plate. The specimens were named as Specimen L-T, S-T, T-L, and R-L by the crack growth direction as listed in Table1.

Figure 3 shows the cutting procedure of specimens from the rolled bar. The tests were carried out under a constant load amplitude, ΔP = 11.8kN with R = -1 and at a frequency 6 Hz.

Specimen and experimental method for Mode III fatigue crack growth test

Figure 4 shows the shape and dimension of the specimen. The specimen was cut in the rolling direction from the rolled bar. A tension-compression-torsion biaxial testing machine was used. In order to introduce a circumferential pre-crack of about 200 μm in depth tension-compression fatigue tests were carried out at σ_a = 150 MPa. The specimens were annealed in a vacuum at 600°C for 1 hr again to relieve the prior fatigue history introduced in the tension-compression test. Torsional fatigue tests were carried out by using the circumferentially cracked specimens under a constant torque amplitude at a frequency 5~12 Hz with zero mean stress.

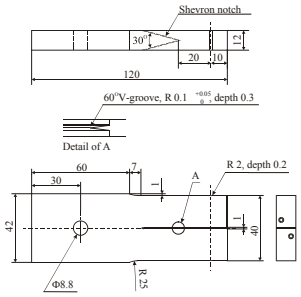

Figure 1: Shape and dimensions of Mode II fatigue crack growth test specimen (mm).

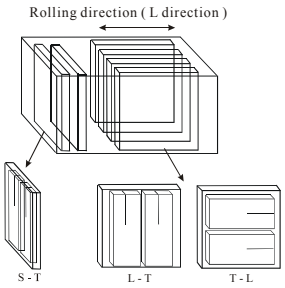

Figure 2: Mode II fatigue crack growth test specimens cut from the plate.

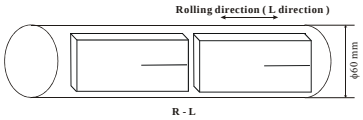

Figure 3: Mode II fatigue crack growth test specimens cut from the rolled bar.

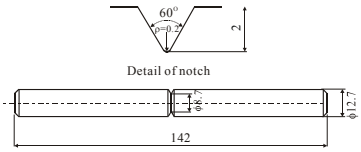

Figure 4: Mode III fatigue crack growth test specimen (mm).

EXPERIMENTAL RESULTS AND DISCUSSION

Fracture surface of Mode II fatigue crack growth

Figure 5 shows the fracture surface produced by Mode II fatigue crack growth in Specimen R-L. The particular feature of the fracture surface is fibrous patterns parallel to the direction of shear stress.

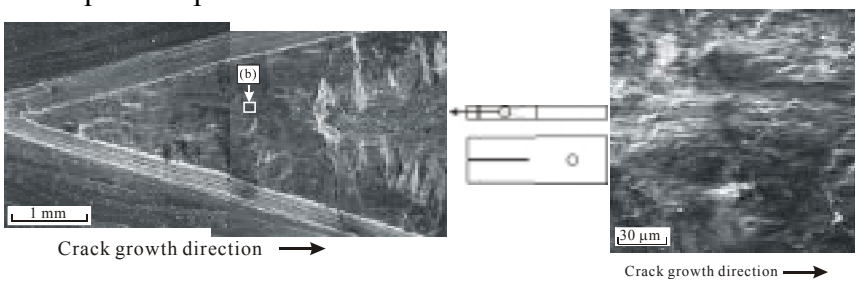

(a) (b)

Figure 5: Fracture surface of Mode II fatigue crack growth observed in Specimen R-L, ΔP = 11.8 kN. (b) is the higher magnification of (a).

Characteristics of Mode II fatigue crack growth

Figure 6 shows the profile of Mode II fatigue crack revealed by sectioning the center of Specimen R-L after the test. In the present Mode II fatigue crack growth test, the value of ΔK_{II} at the crack tip decreases monotonically as Mode II fatigue crack grows [1-3]. After ΔK_{II} reaches ΔK_{IIth}, Mode II fatigue crack growth is stopped and the crack starts to branch to the direction for Mode I growth. This process occurs due to the relationship of $\Delta K_{IIth} > \Delta K_{Ith}$ [2-3]. The branching angle of branched cracks is approximately ± 70.5° to Mode II fatigue crack growth direction [6].

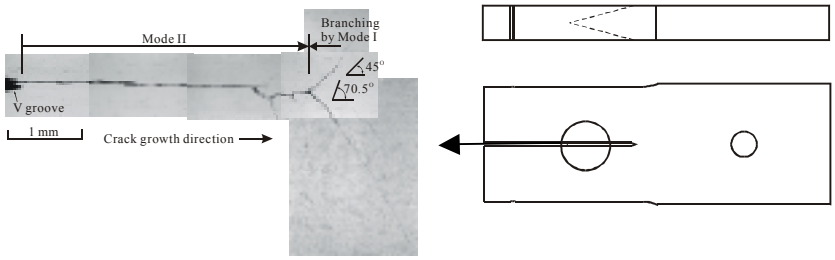

Figure 6: Mode II fatigue crack growth in Specimen R-L. ΔP = 11.8 kN.

Microstructural change in the vicinity of Mode II fatigue crack.

Figure 7(a) shows the microstructure in the vicinity of Mode II fatigue crack of Specimen R-L etched with a nital. It is interesting that darkly etched layers are attached to the surfaces of Mode II fatigue crack. The average value of Vickers hardness HV measured with a load of 0.0029 N at 5 points in the layers of the microstructural change is HV = 468. The value is much higher than that of the original matrix, HV = 164.

Figure 7(b) shows the AFM image of the layers which consists of very fine grains with radius ranging from 100 to 200 nm.

Considering the Hall-Petch type relationship, $HV = C_1 + C_2 \cdot d^{-1/2}$ (d : grain size, C_1 and C_2 are material constants) [7], it is presumed that the extremely fine grain size in the darkly etched layers caused the very high Vickers hardness.

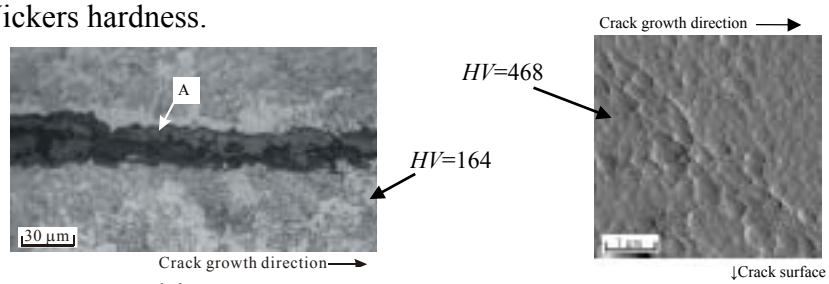

(a) (b) AFM image in the region A in (a)

Figure 7: Microstructural change in the vicinity of the fracture surfaces of Mode II fatigue crack in Specimen R-L. ΔP = 11.8 kN.

Values of ΔK_{IIth} for specimens cut from different directions

Table 1 lists the values of ΔK_{IIth} for the different directions in respect to the rolling direction.

TABLE 1: Values of ΔK_{IIth} and ΔK_{Ith} [MPa$\sqrt{m}$].

Specimen	ΔK_{IIth}	ΔK_{Ith}
L-T(crack growth normal to rolling direction)	9.5	7.8 [8]
S-T(crack growth normal to rolling direction)	9.7	
T-L(crack growth parallel to rolling direction)	8.8	
R-L(crack growth parallel to rolling direction)	8.1	

Fracture surface of Mode III fatigue crack

Figure 8 shows the macroscopic Mode III fracture surface of the specimen tested at ΔK_{III} = 11.5 MPa$\sqrt{m}$. The fracture surface presents a typical morphology of the factory roof. Figure 8(b) shows the mechanism of the formation of the factory roof [9]. Prior to the formation of factory roof, many small semi-elliptical cracks are nucleated by Mode III loading ahead of the initial circumferential crack tip.

Figure 9 shows the fracture surface of the specimen tested at ΔK_{III} = 16.1 MPa$\sqrt{m}$. Figure 9(b) shows the fibrous morphology in parallel to the direction of shear stress. The fibrous morphology produced by Mode III fracture is clearer than that of Mode II fracture surface of Fig.5(b).

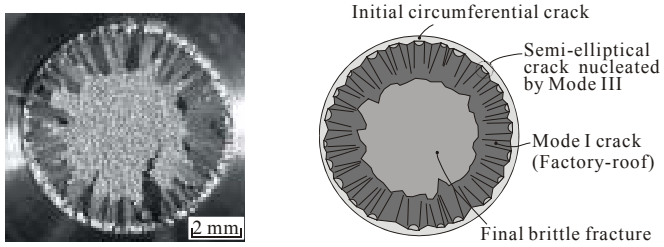

Figure 8: Macroscopic Mode III fracture surface. ΔK_{III} = 11.5 MPa$\sqrt{m}$. (a) Fracture surface morphology of Mode III test specimen. (b) Formation mechanism of the factory roof.

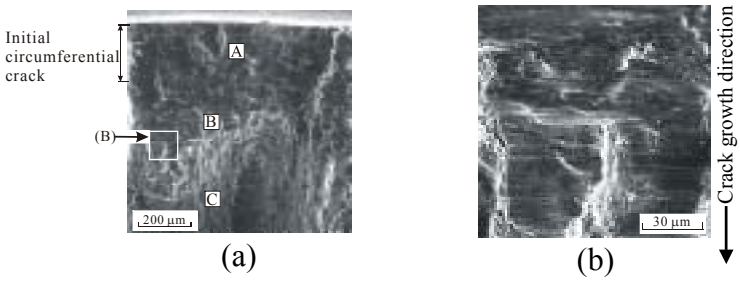

Figure 9: Fracture surface of Mode III fatigue crack growth. ΔK_{III} = 16.1 MPa$\sqrt{m}$. (a) Mode III fracture surface, A: Initial circumferential crack, B: Mode III crack, C: Mode I crack (Factory roof). (b) Fibrous morphology of the Mode III fatigue crack growth (Higher magnification of (a)).

Characteristics of Mode III fatigue crack growth

Figure 10 shows the feature of the Mode III fatigue crack growth of the specimen tested at ΔK_{III} = 13.6 MPa$\sqrt{m}$. Figure 10(a) illustrates the

procedure of turning and polishing the specimen 530 μm in depth from the notch bottom. After turning and polishing, the vicinity of crack was etched with a nital. Branching from the Mode III fatigue crack to the direction of Mode I growth as the case of Mode II fatigue crack (Fig. 6) is revealed. The branching angle is approximately equal to ± 70.5° as Fig.6.

Microstructural change in the vicinity of Mode III fatigue crack

Figure 10(c) shows a microstructural change which looks dark compared to the original microstructure. The average value of Vickers hardness measured with a load of 0.098 N at 5 points at the layer of microstructural change is HV = 678 which is much higher than the hardness of the original matrix HV = 175. It is presumed that the very fine grain size caused the increase in HV at the layer of microstructual change as the case in Fig.7(b).

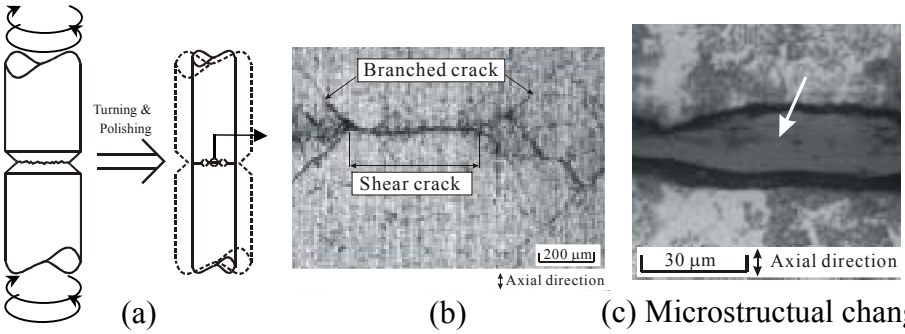

(a) (b) (c) Microstructual change, the dark layers indicated by the arrow.

Figure 10: Mode III fatigue crack growth. ΔK_{III} = 13.6 MPa$\sqrt{\text{m}}$.

Relationship between ΔK_{III} and N_f

Figure 11 shows the relationship between ΔK_{III} and N in the Mode III fatigue crack growth test. The nominal values of ΔK_{III} were calculated by Benthem et al's equation [10] based on the depth of the circumferential crack, b, which was defined by the sum of notch depth, t, and the depth of initial crack, h, and the nominal shear stress at the minimum cross section.

The data with the solid mark ● in Fig.11 shows the specimen in which factory roof was not formed and the data with open mark ○ were those of specimens in which factory roof was formed.

Depth of shear fatigue crack, h_{III} and ΔK_{IIIth}

Figure 12 shows the relationship between h_{III} and ΔK_{III} in the specimens in which factory roof was formed. The values of h_{III} were defined by the depth of shear fatigue crack from the initial crack tip to the maximum depth of

shear crack as shown in Fig.12(b). To evaluate the critical stress intensity factor range for Mode III crack initiation, Mode III stress intensity factor range termed by ΔK^*_{III} was calculated by assuming $b = t + h + h_{III}$. Figure 13 shows the relationship between $(\Delta K^*_{III} - \Delta K_{III}) / \Delta K_{III}$ and ΔK_{III} (the nominal stress intensity factor ranged defined by the initial crack depth.). The values of $(\Delta K^*_{III} - \Delta K_{III}) / \Delta K_{III}$ decrease with the decrease in the values of ΔK_{III}. For $\Delta K_{III} = 9.6$ MPa$\sqrt{\text{m}}$, $(\Delta K^*_{III} - \Delta K_{III}) / \Delta K_{III}$ is negligibly small. It means that the difference between ΔK^*_{III} calculated by $b = t + h + h_{III}$ and ΔK_{III} calculated by $b = t + h$ is small enough to consider that the value of h_{III} = 260 μm (see Fig. 12(a)) at $\Delta K_{III} = 9.6$ MPa$\sqrt{\text{m}}$ does not influence the value of ΔK^*_{III}. Thus, it is presumed that the Mode III fatigue crack stopped and branched to the direction for Mode I growth (factory roof) after the shear crack reached the depth h_{III} = 260 μm at $\Delta K_{III} = 9.6$ MPa$\sqrt{\text{m}}$. Therefore, it may be concluded that $\Delta K_{IIIth} \cong 9.6$ MPa$\sqrt{\text{m}}$. Table 1 shows that ΔK_{IIth} = 9.5 MPa$\sqrt{\text{m}}$ for Specimen L-T and 9.7 MPa$\sqrt{\text{m}}$ for Specimen S-T, and the average value is $\Delta K_{IIth} \cong 9.6$ MPa$\sqrt{\text{m}}$ for crack growth to the normal direction to the rolling direction. Thus, the value of ΔK_{IIth} is approximately equal to the value of ΔK_{IIIth} for 0.47 % carbon steel (JIS S45C), and accordingly the mechanism of Mode II fatigue crack growth is presumed to be essentially identical to that of Mode III fatigue crack growth.

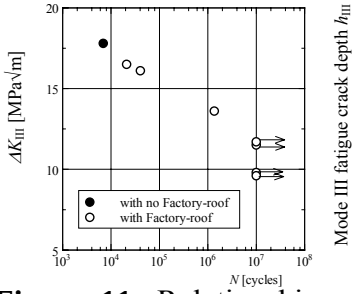

Figure 11: Relationship between ΔK_{III} and N.

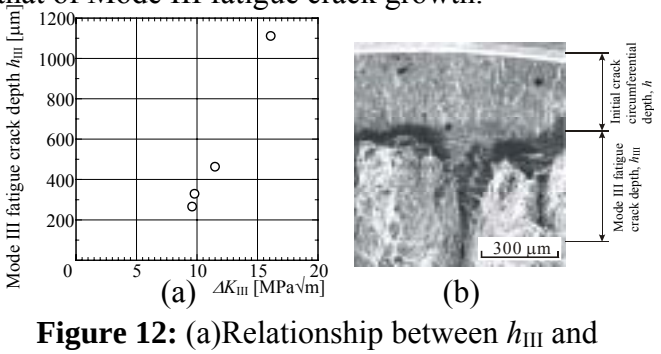

Figure 12: (a)Relationship between h_{III} and ΔK_{III}. (b) Definition of Mode III fatigue crack depth, h_{III}.

Figure 13: Relationship between $(\Delta K^*_{III}-\Delta K_{III}) / \Delta K_{III}$ and ΔK_{III}. ΔK_{III}: the nominal Mode III stress intensity factor range. ΔK^*_{III} : The ΔK value for crack depth = notch depth (t) + initial crack depth (h).

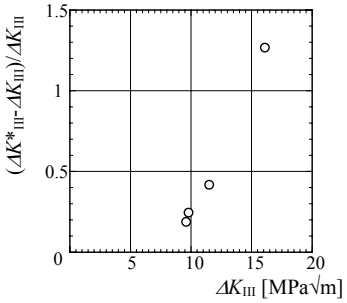

CONCLUSION

In order to make clear the relationship between ΔK_{IIth} and ΔK_{IIIth} and the influence of the rolling texture, Mode II and Mode III fatigue crack growth tests were carried out for annealed 0.47 % carbon steels (JIS S45C). The following conclusions were derived.

(1) The values of ΔK_{IIth} for crack growth normal to the rolling direction are higher than ΔK_{IIth} for crack growth parallel to the rolling direction.

(2) Mode II and Mode III fatigue crack growth produced darkly etched microstructural layers in the vicinity of Mode II and Mode III fatigue crack. Vickers hardness of the layers was much higher than the original matrix (Mode II: *HV* 164 → *HV* 468. Mode III: *HV* 175 → *HV* 678). The layers consisted of very fine grains ranging from 100 to 200 nm.

(3) ΔK_{IIth} was approximately equal to ΔK_{IIIth}, i.e. $\Delta K_{IIth} \cong \Delta K_{IIIth} \cong 9.6$ MPa$\sqrt{\text{m}}$ for crack growth perpendicular to the rolling direction.

REFERENCES

1. Y. Murakami, S. Hamada, K. Sugino and K. Takao (1994) Journal of Materials Science, Japan, 43-493, p.1264.
2. Y. Murakami and S. Hamada (1997) Fatigue Fract. Engng Master. Struct., 20-6, p.863.
3. Y. Murakami, C. Sakae and S. Hamada (1999) In: Engineering Against Fatigue, pp.473-485, J. H. Baynon, M. W. Brown, T. C. Lindley, R. A. Smith, and B. Tomkins, (Eds). A. A. Balkema, Rotterdam
4. R. O. Ritchie, F. A. McClintock, H. Nayeb-Hashemi and M. A. Ritter (1982) Metal. Trans, 13A, p.101.
5. E. K. Tschegg (1983) J. Mater, Sci, 18, p.1604.
6. F. Erdogan, G. C. Sih, (1963) J. Bas. Engng Trans. ASME, 85, 519.
7. Y. Kimura and S. Takaki (1995) Mater. Trans. JIM, 36-2, p.289.
8. Y. Murakami and K. Matsuda (1986) Trans. of the Japan Society of Mechanical Engineers A52-478 p.1492.
9. K. Takahashi and Y. Murakami (2001) Proc. 6th Int. Conference Biaxial / Multiaxial Fatigue & Fracture, vol.2, p.581.
10. J. P. Benthem and W. T. Koiter (1973) In: Stress Intensity Factors Handbook, Vol.3, p.663, Y. Murakami et al (Ed.). The Society of Materials Science, Japan, Kyoto & Pergamon Press, Oxford.